Formatted: Superscript

Formatted: Superscript

Formatted: Superscript

Journal Name

COMMUNICATION

Square-planar Co(III) in {O₄} Coordination: Large ZFS and Reactivity with ROS

Received 00th January 20xx, Accepted 00th January 20xx

DOI: 10.1039/x0xx00000x

Jennifer L. Steele, a Laleh Tahsini, a Chen Sun, a Jessica K. Elinburg, a Christopher M. Kotyk, a James McNeely, ^a Sebastian A. Stoian, ^b Alina Dragulescu-Andrasi, ^d Andrew Ozarowski, ^c M. Ozerov, ^c J. Krzystek, ^c Joshua Telser, ^f Jeffrey W. Bacon, ^a James A. Golen, ^e Arnold L. Rheingold, e and Linda H. Doerrera,

Oxidation of distorted square-planar perfluoropinacolate Co compound $[Co^{II}(pin^F)_2]^{2-}$, 1, to $[Co^{III}(pin^F)_2]^{1-}$, 2, is reported. Rigidly square-planar 2 has an intermediate-spin, S = 1, ground state and very large zero-field splitting (ZFS) with $D = 67.2 \text{ cm}^{-1}$; |E| = 18.0cm⁻¹ (*E/D*) = 0.27, g_{\perp} = 2.10, g_{\parallel} = 2.25 and χ_{TIP} = 1950·10⁻⁶ cm³/mol. This Co(III) species, 2, reacts with ROS hydroxyl radicals to oxidise two (pinF)2- ligands to form tetrahedral [Coll(Hpfa)4]2-, 3.

Metal complexes supported by oxidatively robust ligands are crucial to many catalytic transformations including water remediation,1 water oxidation,2-4 and selective C-H bond oxidation. 5-8 One approach that engenders oxidative resistance is to use extensively fluorinated ligands. Chelating bidentate ligands have additional stability vs. two monodentate ligands, and $H_2 \text{pin}^\text{F}\text{, perfluoropinacol, is of particular interest because its}$ complexes can routinely be prepared in water ($pKa_1 = 6.05$, pKa_2 = 10.7, titration in Figure S1). Homoleptic 3d complexes $[M(pin^F)_2]^{2-}$ with M = Fe - Zn have been reported^{9, 10} including [Me₄N]₂[Co(pin^F)₂], 1 (Scheme 1), which binds CH₃CN but not THF in solution. 10 Reactivity with O2 for this Co species was also reported,11 the conclusions from which we have come to doubt as discussed below

Compound 1 is stable for days in aqueous solutions as the five coordinate adduct $[Co(OH_2)(pin^F)_2]^{2-}$ when buffered between pH 9 – 11 with $(pin^F)^{2-12}$ In contrast, CH₃CN solutions of 1 in air undergo distinct colour changes in hours. The pink $\boldsymbol{1}$ ($\lambda_{\text{max}},$ nm $(\epsilon, M^{-1}cm^{-1})) = 505 (27), 560 (43)), converts to a bright$ yellow/orange species with an intense absorption at 405 nr (3790), 2, and then ultimately transforms to a violet species, $(\lambda = 481 (133), 567 (165))$ in ~ 95% yield after five days (Figure S2). Purple X-ray quality crystals were obtained by layering Et₂O onto violet acetone solutions, enabling identification of the pseudo-tetrahedral complex $[Me_4N]_2[Co^{II}(Hpfa)_4]$, 3. The metal centre is bound by four monodentate alkoxide ligands, designated (Hpfa)- for the monodeprotonated form of the perfluoroacetone geminal diol, H₂pfa (Scheme 1 and Figure 1). As noted, the conversion of 1 to 3 in CH₃CN under aerobic conditions passes through an orange intermediate, 2, with a strong absorbance at 405 nm. Efforts to isolate the orange species from this reaction mixture were unsuccessful. The composition of 3 suggests that four equiv of hydroxyl radical, HO*, are formally required for its formation. Therefore, we treated 1 with H2O2 trying to prepare a posited {Co(III)-OH} species. Adding one equiv of H₂pin^F to **1** in wet CH₃CN, followed by one equiv of H₂O₂, affords an absorbance increase at 405 nm over an hour (Figure 2). Next, the ligand-cleaved product 3 can be formed by adding one equiv of Me₄NOH to **2** following its full

- a Chemistry Department, Boston University, 590 Commonwealth Ave., Boston, MA 02139 USA.

 Department of Chemistry, University of Idaho, 875 Perimeter Drive, MS 2343,
- Moscow, ID 83844, USA
- National High Magnetic Field Laboratory, Florida State University, 1800 E. Paul
- Dirac Drive, Tallahassee, Fl. 32310, USA

 *Department of Chemistry and Biochemistry, Florida State University, 95 Chieftan
 Way, Tallahassee, Fl. 32306, USA

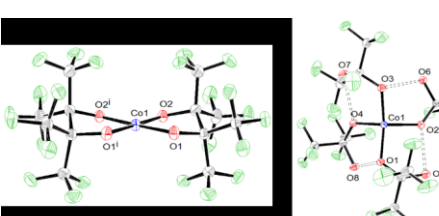
 *Department of Chemistry and Biochemistry, University of California, San Diego,
- 9500 Gilman Drive, MC 0332, La Jolla, CA 92093, USA,
- To Department of Biological, Chemical and Physical Sciences, Roosevelt University, Chicago, IL 60605, USA

 tootnotes relating to the title and/or authors should appear here.

Electronic Supplementary Information (ESI) available including the Experi Section and CIFs for 2 (1407677) and 3 (1407676) via the CCDC. See DOI:

10.1039/x0xx00000x † Footnotes relating to the title and/or authors should appear here

Electronic Supplementary Information (ESI) available: [details of any supplementary information available should be included here]. See DOI: 10.1039/x0xx00000x



formation (Figure S3). Isolation

Figure 1. ORTEPs of anions of 2 (left) and 3 (right). Dotted lines indicate hydrogen bonding interactions.

This journal is © The Royal Society of Chemistry 20xx

J. Name., 2013, **00**, 1-3 | **1**

COMMUNICATION Journal Name



Scheme 1. Formal interconversions of anions $[Co(pin^{f})_{2}]^{2}$, 1, $[Co(pin^{f})_{2}]^{1}$, 2, and $[Co(Hpfa)_{d}]^{2}$. 3

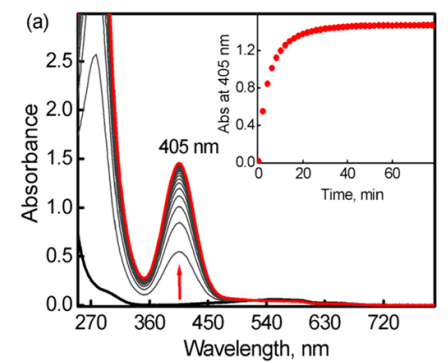
of a posited Co(III) intermediate was not achieved from this reaction, due to an additional pathway that led to an insoluble brown solid and complete loss of product after 24 h. Conversion of $\bf 1$ to $\bf 2$ occurs at a faster rate in the presence of larger amounts of hydrogen peroxide.

Analytically pure $\boldsymbol{2}$ was obtained by oxidizing $\boldsymbol{1}$ under N_2 with AgPF₆ in THF/CH₃CN to yield the surprising square-planar Co(III) species [Me₄N][Co^{III}(pin^F)₂]. The UV-vis spectrum of 2 has an LMCT band at λ_{max} = 405 nm (ϵ = 3790 M⁻¹cm⁻¹). The solutionbased, Evans method $^{\rm 13\text{-}15}$ room-temperature magnetic moment of 3.63 μ_{B} for $\boldsymbol{2}$ suggests an S = 1, intermediate-spin state. This observation is consistent with other Co(III) square planar compounds with $\{N_4\}$, $^{16\cdot19}$ $\{S_4\}$, 20 , 21 $\{C_4\}$, 22 and heteroleptic 23 coordination (summary in Table S1). X-ray quality crystals were obtained by layering a THF solution onto CH₂Cl₂ (Figure 1 and Table S3). The square planar coordination with τ_4 = 0.03 has Co-O bond lengths (1.8020(17) and 1.7995(18) Å) shorter than the average (1.962(3) Å) in 1, as expected. 10 Notably, the UV-vis spectra in both coordinating and non-coordinating solvents are virtually identical (Figure S4), indicating that there is no axial ligand bound in 2 in solid state or in solution. Even when hydroxide is added to 2, no coordination is observed, suggesting a steric, not electronic, reason for unsaturation. The combination of shorter Co-O bonds and the steric bulk of eight CF₃ groups is proposed to inhibit coordination of a fifth ligand. Addition of O₂ to [nBu₄N]₂[Co(pin^F)₂] in "acidified" solution has previously been reported to give a product with a λ_{max} of 405 nm.11 Therein the product was proposed to be the high-spin cobalt(II) species $[^nBu_4N][Co(pin^F)(Hpin^F)(O_2)]\cdot EtOH$ based on a solution magnetic moment measurement and EPR data. 11 Our attempts to repeat the isolation of this product by this method have proved unsuccessful. Because $\boldsymbol{2}$ has an identical $\lambda_{\text{max}},$ similar light sensitivity, and similar magnetic moment to that reported earlier,11 we suggest that the proposed formula11 is incorrect, and that the previously reported compound was ("Bu₄N)+ salt of [Co^{III}(pin^F)₂]¹⁻.

Compound 2 incorporates a rare, paramagnetic Co(III) ion. The room-temperature $^1\text{H-NMR-derived}$ magnetic moment of 2 is corroborated by SQUID magnetometry on a solid sample. Figure 3 shows $\chi T \simeq 1.8$ cm³-K/mol at 300 K corresponding to an apparent effective magnetic moment of 3.78 μ_B . These values are intermediate between those expected for a triplet ($\chi T \approx 1$ cm³-K/mol) and a quintet spin state ($\chi T \approx 3$ cm³-K/mol). From 300 to 50 K, χT gradually decreases, followed by a more dramatic fall to nearly zero at very low temperature. This behaviour suggests the presence of a large temperature independent paramagnetic (TIP) contribution and a large zero-field splitting (ZFS) at low temperature. Least squares fitting of experimental data yielded a ZFS such that $|D| \sim 70$ cm³-f, $E/D \sim 1/3$, $g_{150} = 2.24$ and $\chi_{TIP} = 1950\cdot10^{-6}$ cm³/mol. The

observation of a triplet ground state with this large ZFS is corroborated by reduced magnetization data (inset of Figure 3 and Figure S5), and lack of an EPR signal regardless of temperature even for frequencies as high as 600 GHz (hv = 20) cm⁻¹).²⁴ The ZFS was directly measured by FIRMS (Far InfraRed Magnetic Spectroscopy),²⁵ which detected two resonances in zero field at 49.2 cm⁻¹ and 85.2 cm⁻¹, identified as D-E and D+E transitions, respectively (Figure 4) and leading to |D| = 67.2cm⁻¹; |E| = 18.0 cm⁻¹. The 2E transition, which should appear at 36 cm⁻¹, was not observed and therefore the sign of D is likely to be positive. The positive sign of D is also supported by magnetic fits (Figure S5) and is predicted by second-order perturbation theory using the electronic structure discussed below. Together these observations reveal a large unquenched orbital momentum and a spin-orbit mixing of the orbital ground state with several low-lying orbital states.

Figure 2. UV-vis spectral changes of conversion of 1 to 2 effected by H₂O₂ in CH₂CN



solution. Inset shows the time course of this process.

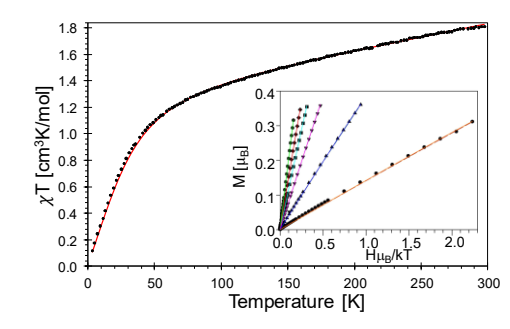
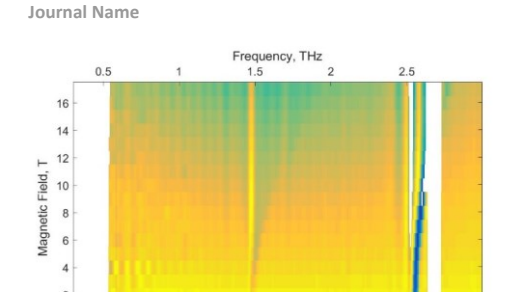


Figure 3. Plot of χT vs. temperature recorded for a powder sample of 2. Shown in black are experimental data points. The solid red line is a simulation obtained for S=1 with D=70 cm⁻¹, E/D=0.33, $g_{loc}=2.24$, and $\chi_{TIP}=1950\cdot10^6$ cm⁻³/mol. The inset shows the reduced magnetization data recorded at 1.7 K, 5 K, 10 K, 15 K, 20 K, and 30 K for fields from 0 to 7 T. The solid lines are simulations obtained using D=65.44 cm⁻¹, E/D=0.33, $g_{loc}=2.22$.



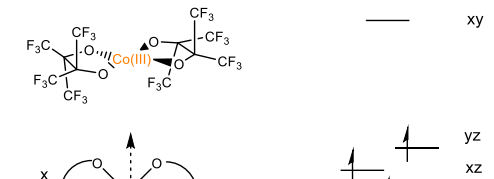
Energy, cm⁻¹

Figure 4. A false colour map of FIRMS resonances at 5 K showing two zero-field transitions at 49.2 cm⁻¹ and 85.2 cm⁻¹ evolving into powder patterns with applied magnetic field. More details can be found in Figures S6-7 in the SI.

To illuminate the nature of the paramagnetic ground state and to rationalize the observed spectroscopic behaviour, we have completed a detailed theoretical investigation of **2**. Calculations using ORCA²⁶ revealed the ligand field splitting shown qualitatively in Scheme 2 (right).

An intermediate-spin, triplet ground state is further supported by triplet (32, 0.0 kcal/mol), singlet (12, 38.9 kcal/mol), and quintet (52, 15.8 kcal/mol) structures optimized at the PBEO/cc- $\ensuremath{\mathsf{pVTZ/RIJCOSX}}$ level of theory. These calculations not only yield a triplet configuration lowest in energy, but a geometryoptimized structure with the best structural agreement with ${\bf 2}$ (Table S4). The spin density for 32 is localized on the Co atom (Figure S8) with the SOMOs best described as $3d_{xx}$ and $3d_{yx}$ orbitals. Analysis of the electron distribution suggests that the $3d_{z^2}$ and $3d_{x^2-y^2}$ orbitals are doubly occupied and that, to a first approximation, the $|(x^2-y^2)^2(z^2)^2(xz)^{\alpha}(yz)^{\alpha}|$ Slater determinant describes best the ground state of 2. This electronic structure is confirmed by NEVPT2(12,10) calculations (Figure S14). The cobalt spin population was 1.80/1.94 in the PBEO/NEVPT2(12,10) calculations for 2 and 1.80/1.95 for 32 based on Löwdin population analysis. This result is a similar electronic structure to that reported in Co complexes with redox-active benzene dithiolate²⁷ and aminophenolate ligands.28

To predict magnetic properties, NEVPT2 calculations were performed on top of CASSCF(12,10) references averaged over the three lowest triplet roots for **2** (see ESI). The axial ZFS parameter D, rhombicity ratio E/D, and isotropic g-value were calculated to be 77.1 cm⁻¹, 0.27, and 2.37 respectively. These theoretical values compare well with experiment. The g-tensor was calculated to be highly anisotropic with principal components $g_z = 2.00$, $g_x = 2.43$, and $g_y = 2.67$. The 3B_2 state (D_2 symmetry, 2273 cm⁻¹) is dominated by configurations characterized by $3d_{x^2}$ to $3d_{xx}$ (72.0%) and $3d_{x^2-y^2}$ to $3d_{xx}$ (22.1%) excitations. The 3B_3 state's (3802 cm⁻¹) dominant configurations are characterized by $3d_{z^2}$ to $3d_{yz}$ (72.0%) and $3d_{x^2-y^2}$ to $3d_{yz}$ (22.1%) excitations.



COMMUNICATION

Scheme 2. Coordinate system used for the discussion of 2 along with a qualitative ligand field splitting diagram derived from NEVPT2(12,10) calculations averaged over three triplet states. NOs and NOONs can be found in Figure S26.

These quantum chemical theory calculations were complemented by a series of classical ligand field theory calculations that determined $D\approx 70~{\rm cm}^{-1}$ with evidence that contributions from both quintet and singlet excited states are required for quantitative agreement with experiment, but the dominant contribution is from triplet excited states arising from transitions from the $3d_{x^2}$ and $3d_{x^2-y^2}$ orbitals to the $3d_{xz}$ and $3d_{yz}$ orbitals (details in ESI).

To understand the formation of $\bf 3$ via $\bf 2$, $\bf 1$ was reacted with O_2 , H_2O , and H_2O_2 . Compound 1 is stable up to pH = 11,¹² and therefore nucleophilic attack by hydroxide alone does not lead to C-C bond cleavage in neutral water; some oxidation is required. There is no appearance of 2 or conversion to 3 from the addition of H₂O or O₂ alone to 1, but 1 reacts with O₂ in the presence of a mild acid such as H2pinF. This reaction slowly afforded 2, but in significant yield only after four days, and complete conversion to 3 took seven days (Figure S17). When 2 in dry CH₃CN is exposed to air in the presence of (nBu₄N)PF₆, it is slowly converted to 3 as indicated by UV-vis spectroscopy (Figure S18), with a competing pathway leading to an insoluble brown precipitate. Starting with dry CH₃CN and gradual exposure to air, the conversion from 2 to 3 takes up to a month and also shows conversion to a transient Co(II) species after 24 h. This Co(II) species could be 1, which is produced from a solution of ${f 2}$ when exposed to light under N_2 (Figure S18). These observations suggest that both the oxidant O2 and a source of H+ are necessary for the formation of 2, and a further ROS is needed to form ${\bf 3}$. The fact that ${\bf 2}$ does not form in H_2O suggests a radical species whose lifetime is greater in CH₃CN than H₂O. Isotopic labelling experiments were conducted to determine the source of the new OH groups in the (Hpfa): ligands, Each of ¹⁸O₂ and H₂¹⁸O was separately introduced to a solution of 1, while the other component was kept unlabelled, and 3 formed in CH₃CN. The product 3 was recrystallized and analysed by ESI-MS (Figures S19-21) which showed ¹⁸O in [Co(Hpfa)₄]²⁻ from both reactions. These data and the H₂O₂ experiment suggest a reactive oxygen species, such as HO•, that can form in more than one way. Because oxidation is required, O2 could be responsible for HO• formation, either indirectly from water oxidation, or directly from itself being converted to hydroxyl radical (Scheme S1).

COMMUNICATION Journal Name

Redox behaviour was also investigated with cyclic voltammetry (CV). Compound **1** showed a quasi-reversible Co^{3+}/Co^{2+} couple with an E_{1/2} of -0.134 V vs Fc'/Fc (Figure S22). Under N₂, **2** showed a reversible couple with an E_{1/2} of -0.167 V vs. Fc/Fc⁺, and when **3** was studied in dry CH₃CN under N₂, a widely-separated redox couple is observed, as well as another oxidation event (Figure S23).

The reactivity of these species was monitored by cyclic voltammetry: In CH_3CN under ambient conditions both electrochemical and UV-Vis data confirm the completion of the reaction of 1 to 3 within several hours (Figure S24). However, under ambient conditions in CH_3CN no conversion of purified 2 to 3 was observed within one day, which is consistent with our previously noted UV-Vis experiments

Interestingly, the CV of **3** in wet CH₃CN shows oxidative catalytic current (Figure S25), which increases with subsequent additions of H_2O until a solid blue precipitate forms. Controlled potential electrolysis, shows that the initial oxidative current significantly diminished after 750 s. and did not increase when H₂O was added at 1800 s. When the working electrode was placed in fresh electrolyte (Figures S26 and S27) little activity was observed indicating that there was not an active heterogeneous film. This catalytic activity may be water oxidation by nanoparticulate CoO_v material, a known H₂O oxidation catalyst,30 for which 3 is a precursor in CH3CN. Little change was observed in CV data when the solution was filtered (Figure S28). In summary, a highly unusual square-planar, paramagnetic Co(III) species, [Co(pin^F)₂]¹⁻, **2**, has been prepared from [Co(pin^F)₂]²⁻ by two different routes. Compound 2 has an intermediate-spin, S = 1, ground state and very large ZFS with $|D| \simeq 70$ cm⁻¹, $E/D \simeq 1/3$, $g_{\perp} = 2.10$, $g_{\parallel} =$ 2.25 and χ_{TIP} = 1950·10⁻⁶ cm³/mol. This compound reacts with reactive oxygen species to form a new tetrahedral Co(II) compound, $[Co(Hpfa)_4]^{2-}$, 3, encapsulated by four intramolecular hydrogen bonds among four monodentate diolate ligands.

This work was supported by NSF-CHE 1362550 (LHD), DOE-BES DE-FG02-11ER16253 (LHD), Boston University UROP, NSF-CHE 0619339 (BU NMR spectrometer). Part of this work was performed at NHMFL which is supported by the NSF award DMR-1644779 and by the State of Florida. Partial support for AD-A from the NSF (CHE 1464955) and the University of Idaho (SAS) is acknowledged. We thank the referees for useful mechanistic discussions.

Conflicts of interest

There are no conflicts to declare.

Notes and references

 T. J. Collins and A. D. Ryabov, Chem. Rev., 2017, 117, 9140-9162.

- H. Lv, Y. V. Geletii, C. Zhao, J. W. Vickers, G. Zhu, Z. Luo, J. Song, T. Lian, D. G. Musaev and C. L. Hill, *Chem. Soc. Rev.*, 2012 **41** 7572-7589
- J. J. Concepcion, J. W. Jurss, M. K. Brennaman, P. G. Hoertz, A. O. T. Patrocinio, N. Y. Murakami Iha, J. L. Templeton and T. J. Meyer, *Acc. Chem. Res.*, 2009, **42**, 1954-1965.
- P. Du and R. Eisenberg, Energy Environ. Sci., 2012, 5, 6012-6021.
- R. A. Sheldon, I. W. C. E. Arends, G.-J. ten Brink and A. Dijksman, Acc. Chem. Res., 2002, 35, 774-781.
- D. Wang, A. B. Weinstein, P. B. White and S. S. Stahl, Chem. Rev., 2018, 118, 2636-2679.
- S. R. Neufeldt and M. S. Sanford, Acc. Chem. Res., 2012, 45, 936-946.
- B. G. Hashiguchi, S. M. Bischof, M. M. Konnick and R. A. Periana, Acc. Chem. Res., 2012, 45, 885-898.
- S. A. Cantalupo, S. R. Fiedler, M. P. Shores, A. L. Rheingold and L. H. Doerrer, Angew. Chem., Int. Ed., 2012, 51, 1000-1005.
- L. Tahsini, S. E. Specht, J. S. Lum, J. J. M. Nelson, A. F. Long, J. A. Golen, A. L. Rheingold and L. H. Doerrer, *Inorg. Chem.*, 2013, 52, 14050-14063.
- 11. C. J. Willis, J. Chem. Soc., Chem. Commun., 1974, 117-118.
- L. Tahsini, W. P. Carbery, M. Z. Ertem, S. A. Cantalupo, J. A. Golen, A. L. Rheingold, V. S. Batista and L. H. Doerrer, manus in prep, 2018.
- G. A. Bain and J. F. Berry, J. Chem. Educ., 2008, 85, 532-536.
- 14. D. F. Evans, J. Chem. Soc., 1959, 2003-2005.
- 15. S. K. Sur, J. Magn. Reson., 1989, 82, 169-173.
- S. E. Harnung and E. Larsen, *Inorg. Chem.*, 2007, 46, 5166-5173.
- B. Ramdhanie, L. N. Zakharov, A. L. Rheingold and D. P. Goldberg, *Inorg. Chem.*, 2002, 41, 4105-4107.
- L. H. Doerrer, M. T. Bautista and S. J. Lippard, *Inorg. Chem.*, 1997, 36, 3578-3579.
 P. J. M. W. L. Birker, J. J. Bour and J. J. Steggerda, *Inorg.*
- Chem., 1973, **12**, 1254-1259. 20. R. Williams, E. Billig, J. H. Waters and H. B. Gray, *J. Am*.
- Chem. Soc., 1966, 88, 43-50.
 21. F. L. Benedito, T. Petrenko, E. Bill, T. Weyhermüller and K.
- Wieghardt, *Inorg. Chem.*, 2009, **48**, 10913-10925.

 22. M. A. García-Monforte, I. Ara, A. Martín, B. Menjón, M.
- Tomás, P. J. Alonso, A. B. Arauzo, J. I. Martínez and C. Rillo, *Inorg. Chem.*, 2014, **53**, 12384-12395.
- P. O. Lagaditis, B. Schluschaß, S. Demeshko, C. Würtele and S. Schneider, *Inorg. Chem.*, 2016, 55, 4529-4536.
- A. K. Hassan, L. A. Pardi, J. Krzystek, A. Sienkiewicz, P. Goy, M. Rohrer and L.-C. Brunel, J. Magn. Reson., 2000, 142, 300-312.
- J. Ludwig, Y. B. Vasilyev, N. N. Mikhailov, J. M. Poumirol, Z. Jiang, O. Vafek and D. Smirnov, *Phys. Rev. B*, 2014, 89, 241406.
- F. Neese, ORCA An Ab Initio, DFT and Semiempirical SCF-MO Package, Ver. 4.0, Max Planck Institute for Chemical Energy Conversion, Mülheim a. d. Rurh, Germany, 2017, pp.
- K. Ray, A. Begum, T. Weyhermüller, S. Piligkos, J. van Slageren, F. Neese and K. Wieghardt, J. Am. Chem. Soc., 2005, 127, 4403-4415.

4 | J. Name., 2012, **00**, 1-3

This journal is © The Royal Society of Chemistry 20xx

COMMUNICATION Journal Name

- B. Eckhard, E. Bothe, P. Chaudhuri, K. Chlopek, D. Herebian, S. Kokatam, K. Ray, T. Weyhermüller, F. Neese and K. Wieghardt, *Chemistry A European Journal*, 2005, **11**, 204-224. 28.
- 29. J. Bendix, in Comprehensive Coordination Chemistry II, Volume 2: Fundamentals: Physical Methods, Theoretical Analysis, and Case Studies, ed. A. B. P. Lever, Elsevier, Amsterdam, 2003, vol. 2, pp. 673-676.

 X. Deng and H. Tuysuz, *ACS Catalysis*, 2014, **4**, 3701-3714.
- 30.